

Data Analysis of KOMPSAT Thermal Test in Simulated On-orbit Environment

Jeong-Soo Kim*

Satellite Bus Department

Korea Aerospace Research Institute, Yuseong P.O. Box 113, Taejeon, Korea 305-600

Young-Keun Chang**

Department of Aerospace Engineering

Hankuk Aviation University, 200-1 Hwajon-dong, Koyang-city, Kyonggi-do, Korea 412-791

Abstract

On-orbit thermal environment test of KOMPSAT was performed in early 1999. An analysis of the test data are addressed in this paper. For the thermal-environmental simulation of spacecraft bus, an artificial heating through the radiator zones and onto some critical heat-dissipating electronic boxes was made by Absorbed-heat Flux Method. Test data obtained in terms of temperature history were reduced into flight heater duty cycles and converted into the total electrical power required for spacecraft thermal control. Verification result of flight heaters dedicated to the bus thermal control is presented. Additionally, an exhaustive heating-control process for maintaining the spacecraft thermally safe and for realistic simulation of the orbital-thermal environment during the test are graphically shown. Qualitative suggestions to post-test model correlation are given in consequence of the analysis.

Key Word : thermal balance test, absorbed-heat flux method, heater duty cycle

Introduction

KOMPSAT (Korea Multi-purpose Satellite) is a sun-synchronous LEO(Low Earth Orbit) satellite built by the joint-development program of Korea Aerospace Research Institute (KARI) and TRW (Redondo Beach, California, USA). Its Proto-flight Model (PFM) was successfully integrated and tested at TRW by Korean and TRW engineers. The Flight Model (FM) had been integrated at KARI and its functional and environmental test was performed in mid 1999. Aboard a Taurus solid rocket which had been built by OSC (Orbital Science Corporation, USA), it was launched from Vandenberg Air Force Base in California, USA in late 1999, and placed into its circular operational orbit of 685 km altitude and 98 deg. inclination to facilitate the cartography, ocean color imaging, and ionosphere measurement.

In orbit, satellites are exposed necessarily to high vacuum and extremely low temperature of deep space that is 4 K ideally, as well as spatial-environmental heating. The principal forms of environmental heating are sunlight, both direct and reflected off (albedo) of the earth, and IR (infrared) energy emitted from the earth itself. Thermal control of a satellite in orbit is achieved by balancing the energy emitted by the spacecraft as IR radiation against the energy dissipated by internal electrical components plus the energy absorbed from the environment.

* Senior Researcher

** Assistant Professor

To verify the thermal design and to ensure successful operation in the space environment, satellites are to be subjected to extensive ground thermal testing prior to the launch. An US Air Force military standard (MIL-STD-1540B, 1982) establishes a uniform set of definitions, environmental criteria, and test methods for military space vehicles, subsystems, and components. This also states that the test requirements should be tailored to the specific space program, considering design complexity, state of the art, mission criticality, and acceptable risk. Acceptance tests are required formal tests that are conducted to demonstrate performance to specified requirements and to act as quality-control screens to detect deficiencies in workmanship, materials, and quality. Three tests described in MIL-STD-1540B associated with space vehicle level are thermal cycling, thermal vacuum, and thermal balance. The thermal cycling tests at system level, as in the component level, are primarily environmental screens to expose design, workmanship, material, and processing defects. This test is optional at the spacecraft level and usually replaced by thermal vacuum test.

The objective of thermal vacuum test is to expose spacecraft to environments which are nondestructive in nature, but yet able to provide assurance of detecting any deficiencies. This test is constituted primarily of system-level functional performance tests between and at temperature extremes. Emphasis is put on component and subsystem interaction and interfaces, and on end-to-end electrical system performance. Thermal hardware functions such as thermostat and heater actuation as well as thermal control software are also verified during this test. Temperature extremes are based upon worst-case analytic prediction for at least one component in each zone. Typically the spacecraft is divided into manageable zones and the test temperature limits are specified for each zone. A variety of components, often tested to different temperature extremes during component acceptance, must be accommodated during system-level thermal testing. The approach taken is to drive as many components as possible to their acceptance temperature extremes, with the constraints that any component should not exceed its component-level extremes to avoid over-stressing.

Thermal balance test is comprised of dedicated thermal tests conducted during thermal vacuum test to verify the thermal analytic models and the thermal design by way of the functional demonstration of thermal control hardware and software. A successful test and subsequent model correlation establishes the ability of the thermal control subsystem to maintain all payloads and bus equipment within specified temperature limits for all mission phases. Several mission phases such as launch, solar array deployment, sun pointing, science, and safe haven mode, etc. are commonly involved in satellite operation with their specific thermal environments and electrical power on/off configurations. As run-time of thermal facilities is expensive, a judicious choice of test cases should be made. KOMPSAT thermal balance test was performed with two extreme cases of environments and configurations of cold BOL (Beginning-of-Life) Safe Haven Mode and hot EOL (End-of-Life) Science Mode. Hot case falls under high solar energy absorption at EOL of high absorptivity and such high, yet realistic, levels of equipment usage as an active operation of payloads. Minimal equipment usage, bus voltage, and solar heating such as safe haven mode at BOL are the conditions for cold case.

On the ground test, high vacuum and extremely low temperature of spatial environments are achieved by space-simulation chamber equipped with liquid-nitrogen-cooled internal shrouds and cryo-pumps of high capability (Kim et al., 1996). Specific power configuration of spacecraft equipments is made by EGSE (Electrical Ground Support Equipment) through powering and controlling the operational state of all the bus equipments. However, realization of the on-orbit environmental heating is the matter of delicacy.

Simulation methods of environmental heat loads are divided into two categories: absorbed-heat flux and incident-heat flux. With the latter using the solar simulator as an incident flux generator, spectral matching is not exact, and reflection and reradiation sometimes occur from auxiliary equipment within the chamber (Gilmore, 1994). Hot-case conditions often can not be properly simulated because thermally-critical surfaces, e.g., SSM (second surface mirror) as a radiator and/or MLI (multi layer insulation) blanket as radiation insulator, have BOL (new) radiative properties while ground-testing, whereas practical hot cases are dominated by EOL (degraded) properties in orbit. A replacement of the incident flux is the absorbed flux method of low cost and low complexity. This technique

is, however, heavily dependent on analysis for determining the intensity and distribution of environmental heat flux, and there also needs a fairly delicate test engineering in practicing a realistic environmental simulation. Test-only heaters are directly affixed to the spacecraft in this method and the flux to be imposed is managed by a heat-loads control system. Test heaters are taken off after the test and refurbishment should be performed to keep away from any possibility of contamination which could be caused by heater adhesives. Merits and demerits of the above two methods were described in detail in Kim & Cho (1998 & 1999) and there can be found the test-design philosophy, too.

Test implementation by the absorbed flux method is described in this paper. Results analysis is confined to spacecraft bus system: Payload system has its own thermal design and control logics which are decoupled from bus system. Through the thermal vacuum test, during which end-to-end electrical test was comprehensively performed, functioning of hardware and software dedicated to thermal control in mission operation orbit were verified and is presented here. Temperature history obtained for the period of cold/hot thermal balance are reduced into flight-heater duty cycles and subsequently converted into total electrical power.

Test Setup, Test Design, and Verification of Test Equipment

1. Test Configuration

The KOMPSAT spacecraft is placed in a space-simulation chamber with a cryogenic shroud. The shroud is chilled upto the temperature less than $-170\text{ }^{\circ}\text{C}$ with liquid nitrogen to simulate the cold sink of outer space. The condition of high vacuum of 10^{-5} Torr or less is achieved by cryo-pumps. Figure 1 shows KOMPSAT FM spacecraft installed on the mounting fixture of space-simulation chamber whose available diameter/length is 3.6X3.0 m. In order to keep the spacecraft away from unwanted conductive heat sink which can be caused by the fixture, a thermal insulator is inserted in between.

KOMPSAT bus structure consists of a payload module, an electronic equipments module, a propulsion module, and a launch vehicle adapter with two solar array wings. Thermal test of the solar array wings was independently performed at subsystem level and thus the Fig. 1 does not show them. Payload module contains payload platform and six(6) payload enclosure panels. All payload equipment is mounted on both faces of payload platform (ESA, LSA, SPS, FMU, two CES's, and two FSS's on +Z face; EEA, LEA, two X-band transmitters, and CESE on -Z face: Refer to the acronym list on last page of this article). The payload module is attached to the nadir platform of electronic equipments module. The equipments module consists of longerons, rails, nadir and central platform, and six(6) equipment enclosure panels. It equips with most of the spacecraft electronics (four RWA's, three GRA's, and CEA on -Z face of nadir platform; OBC, two ECU's, two RDU's, and PCU on +Z face of central platform; two SADA's, two SAR's, SADE, DDC, two S-band Transponders, and VDE on -Z face of central platform). The propulsion module contains propulsion subsystem and zenith platform. All the panels and platforms are of aluminum-facesheet honeycomb structure.

SSM as a representative radiator adheres to the enclosure panels. The bus enclosure panels are completely covered with MLI only except the SSM or other radiator regions. The MLI insulates the bus from heat flows either into or out of the bus structure, while the SSM allows radiation to space. The SSM's reflect most of the incident solar radiation when they are exposed to the sun and albedo heat loads. SSM of 6 mil thickness has the radiative property that is IR emissivity, $\epsilon = 0.78$, and solar absorptivity, $\alpha = 0.07$ (BOL) to 0.15 (EOL). Environmental heat loads are, by the employment of absorbed-flux method, simulated with strip heaters affixed directly to the radiator zones of twelve enclosure panels of the payload and equipments module. It is shown in the enclosure-panel layout of Fig. 1 (around right-upper corner) that six heater circuits (H1, H3, H6, H9, H12, and H15) were applied to the radiator area of six payload panels, six ones (H2, H4, H7, H10, H13, and H16) to upper equipments module, and five ones (H5, H8, H11, H14, and H17) to lower equipments module.

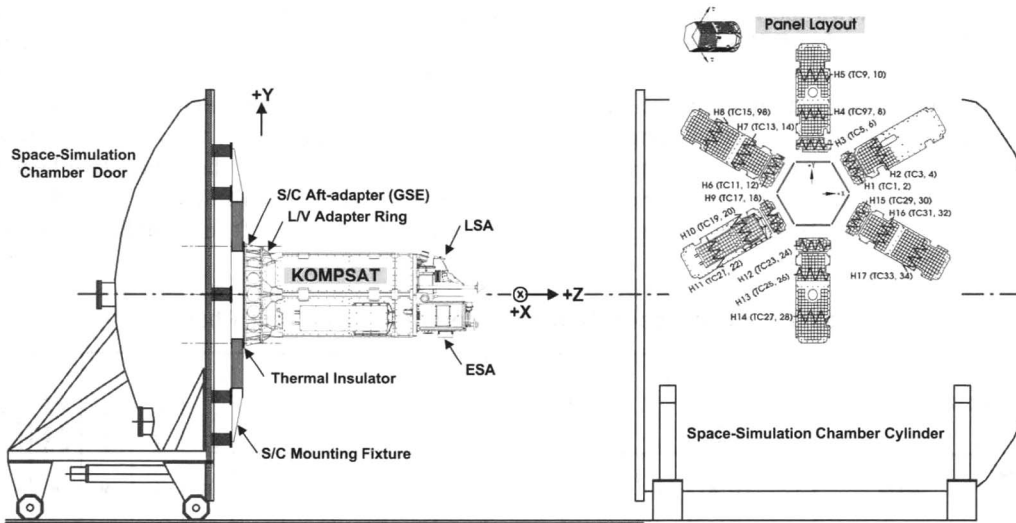


Fig. 1. Configuration of KOMPSAT FM Installed on Space-Simulation Chamber Door

2. Test Design and Instrumentation

Satellite is subjected to three times of thermal vacuum cycling followed by one temperature cycle during which CPT (Comprehensive Performance Test) and thermal balance tests are performed at the cold and hot extremes. Figure 2 schematizes the thermal test time-line. It is shown that the functioning of primary and redundant flight heaters are checked out at the phases of transition toward cold extremes. At the end of three cyclings cold CPT, cold thermal balance, hot CPT, and hot balance test follow and the test ends with system-level leak check of propulsion subsystem.

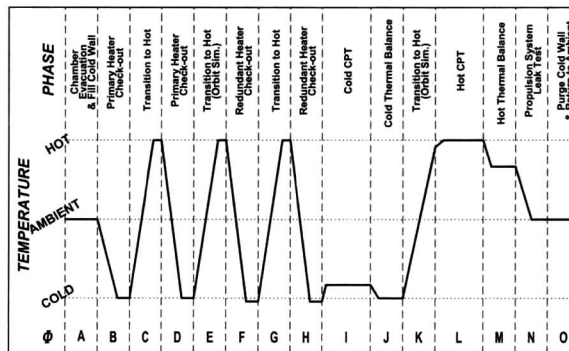


Fig. 2. KOMPSAT Thermal Test Timeline

Table 1 lists control criteria of test heaters practiced through KOMPSAT thermal test. A couple of thermocouples are associated with each heater for providing against single thermocouple fault. Some of the electronics located outside of bus have thermal control surfaces of silverized teflon ($\epsilon = 0.78$, $\alpha = 0.13$ to 0.23). They are FMU, CES's, and GPS receivers, whose environmental heat loads are also to be simulated like as the SSM radiator zones. Besides the radiators there can be found electronics, cables, EGSE's, and mechanical fixtures (MGSE's) to which heating control was made. The heaters accommodated to EGSE's and MGSE's are for guarding against cold environment, and they are maintained to ambient temperature ($20\text{ }^{\circ}\text{C}$) or thereabout.

Figure 3 shows the typical practice of heater application to GSE's and test appendages. H30 and H32 are wrapped to GSE cables which were hooked up to spacecraft from the outside of chamber for electrical functional test. When the cables of large diameter are connected to spacecraft they are cooled down by cold environment and thus may play a role of potential heat sink which lowers the temperature around the connecting area of spacecraft. Since this is not the expected condition in real spacecraft-operational environment, thermal isolation by rendering the conductive heat flux zero ($\nabla T = 0$) is taken to protect the spacecraft against the cool-down influence caused by test appendages. The MGSE's which are directly interfaced to the spacecraft, are similarly controlled with zero-heat flow, too.

Table 1. Heat-Loads Control Criteria for Each Test Phase

S/C Configuration (Phases)			Chamber Evac. & Fill Cold Wall	Primary Heater Checkout	Transition to Hot	Primary Heater Checkout	Transition to Hot	Redundant Heater Checkout	Transition to Hot	Redundant Heater Checkout	Cold CPT	Cold T/B	Transition to Hot	Hot CPT	Hot T/B	Prop. Sys. Leak Test	Purge Cold Wall & Return to Ambient
Heater Ctr. # (Pri.)	Location	Control TC's	A	B	C	D	E	F	G	H	I	J	K	L	M	N	O
H1	+X +Y Payload Radiator	1,2	20±3 °C	Varied	Varied	Varied	Varied	Varied	Varied	Varied	Varied	9.1	Varied	Varied	9.0	20±3 °C	20±3 °C
H2	+X +Y Upper Equip. Rad.	3,4	20±3 °C	Varied	Varied	Varied	Varied	Varied	Varied	Varied	Varied	3.8	Varied	Varied	6.3	20±3 °C	20±3 °C
H3	+Y Payload Rad.	5,6	20±3 °C	Varied	Varied	Varied	Varied	Varied	Varied	Varied	Varied	8.7	Varied	Varied	7.4	20±3 °C	20±3 °C
H4	+Y Upper Equip. Rad.	97,8	20±3 °C	Varied	Varied	Varied	Varied	Varied	Varied	Varied	Varied	3.8	Varied	Varied	5.7	20±3 °C	20±3 °C
H5	+Y Lower Equip. Rad.	9,10	20±3 °C	Varied	Varied	Varied	Varied	Varied	Varied	Varied	Varied	5.2	Varied	Varied	9.6	20±3 °C	20±3 °C
H6	-X -Y Payload Rad.	11,12	20±3 °C	Varied	Varied	Varied	Varied	Varied	Varied	Varied	Varied	9.2	Varied	Varied	9.1	20±3 °C	20±3 °C
H7	-X +Y Upper Equip. Rad.	13,14	20±3 °C	Varied	Varied	Varied	Varied	Varied	Varied	Varied	Varied	2.6	Varied	Varied	4.2	20±3 °C	20±3 °C
H8	-X -Y Lower Equip. Rad.	15,98	20±3 °C	Varied	Varied	Varied	Varied	Varied	Varied	Varied	Varied	7.5	Varied	Varied	12.3	20±3 °C	20±3 °C
H9	-X -Y Payload Rad.	17,18	20±3 °C	Varied	Varied	Varied	Varied	Varied	Varied	Varied	Varied	8.3	Varied	Varied	6.8	20±3 °C	20±3 °C
H10	-X -Y Battery Rad., Upper	19,20	10±3 °C	Varied	Varied	Varied	Varied	Varied	Varied	Varied	Varied	4.5	Varied	Varied	7.3	10±3 °C	10±3 °C
H11	-X -Y Battery Rad., Lower	21,22	10±3 °C	Varied	Varied	Varied	Varied	Varied	Varied	Varied	Varied	6.0	Varied	Varied	9.5	10±3 °C	10±3 °C
H12	-Y Payload Rad.	23,24	20±3 °C	Varied	Varied	Varied	Varied	Varied	Varied	Varied	Varied	7.9	Varied	Varied	3.9	20±3 °C	20±3 °C
H13	-Y Upper Equip. Rad.	25,26	20±3 °C	Varied	Varied	Varied	Varied	Varied	Varied	Varied	Varied	2.2	Varied	Varied	2.5	20±3 °C	20±3 °C
H14	-Y Lower Equip. Rad.	27,28	20±3 °C	Varied	Varied	Varied	Varied	Varied	Varied	Varied	Varied	4.4	Varied	Varied	6.8	20±3 °C	20±3 °C
H15	+X -Y Payload Rad.	29,30	20±3 °C	Varied	Varied	Varied	Varied	Varied	Varied	Varied	Varied	8.5	Varied	Varied	6.8	20±3 °C	20±3 °C
H16	+X -Y Upper Equip. Rad.	31,32	20±3 °C	Varied	Varied	Varied	Varied	Varied	Varied	Varied	Varied	3.8	Varied	Varied	5.7	20±3 °C	20±3 °C
H17	+X -Y Lower Equip. Rad.	33,34	20±3 °C	Varied	Varied	Varied	Varied	Varied	Varied	Varied	Varied	6.5	Varied	Varied	10	20±3 °C	20±3 °C
H18	FMU Radiator	36,35	20±3 °C	Varied	Varied	Varied	Varied	Varied	Varied	Varied	Varied	6.0	Varied	Varied	8.9	20±3 °C	20±3 °C
H19	CES, +Y	37,38	20±3 °C	Varied	Varied	Varied	Varied	Varied	Varied	Varied	Varied	1.9	Varied	Varied	2.6	20±3 °C	20±3 °C
H20	CES, -X	39,40	20±3 °C	Varied	Varied	Varied	Varied	Varied	Varied	Varied	Varied	1.6	Varied	Varied	1.9	20±3 °C	20±3 °C
H21	Xmitter, +X	41,42	Off	Varied	Varied	Varied	Varied	Varied	Varied	Varied	Varied	Off	Varied	Varied	8.6	Off	Off
H22	Xpndr, +X	43,44	Off	Varied	Varied	Varied	Varied	Varied	Varied	Varied	Varied	Off	Varied	Varied	5.5	Off	Off
H23	SAR #1	45,46	Off	Varied	Varied	Varied	Varied	Varied	Varied	Varied	Varied	5.0	Varied	Varied	5.0	Off	Off
H24	SAR #2	47,48	Off	Varied	Varied	Varied	Varied	Varied	Varied	Varied	Varied	5.0	Varied	Varied	5.0	Off	Off
H25	-X -Y Battery Plate	49,50	10±3 °C	Varied	Varied	Varied	Varied	Varied	Varied	Varied	Varied	28.0	Varied	Varied	28.0	10±3 °C	10±3 °C
H26	GPS Receiver A	51,52	20±3 °C	Varied	Varied	Varied	Varied	Varied	Varied	Varied	Varied	3.5	Varied	Varied	0.9	20±3 °C	20±3 °C
H27	GPS Receiver B	53,54	20±3 °C	Varied	Varied	Varied	Varied	Varied	Varied	Varied	Varied	3.5	Varied	Varied	0.9	20±3 °C	20±3 °C
H28	Cable Guard #1 (-Z)	55,56,57	DelT=0	DelT=0	DelT=0	DelT=0	DelT=0	DelT=0	DelT=0	DelT=0	DelT=0	DelT=0	DelT=0	DelT=0	DelT=0	DelT=0	DelT=0
H29	Cable Guard #2 (-Y)	58,59,60	DelT=0	DelT=0	DelT=0	DelT=0	DelT=0	DelT=0	DelT=0	DelT=0	DelT=0	DelT=0	DelT=0	DelT=0	DelT=0	DelT=0	DelT=0
H30	Cable Guard #3 (+X)	61,62,63	DelT=0	DelT=0	DelT=0	DelT=0	DelT=0	DelT=0	DelT=0	DelT=0	DelT=0	DelT=0	DelT=0	DelT=0	DelT=0	DelT=0	DelT=0
H31	Ant. Cables	64,65,66,67	20±3 °C	20±3 °C	20±3 °C	20±3 °C	20±3 °C	20±3 °C	20±3 °C	20±3 °C	20±3 °C	20±3 °C	20±3 °C	20±3 °C	20±3 °C	20±3 °C	20±3 °C
H32	PDTS GSE Cable	84,87	20±3 °C	20±3 °C	20±3 °C	20±3 °C	20±3 °C	20±3 °C	20±3 °C	20±3 °C	20±3 °C	20±3 °C	20±3 °C	20±3 °C	20±3 °C	20±3 °C	20±3 °C
H33	EGSE Unit #4 (BDIFJ)	68,69	20±3 °C	20±3 °C	20±3 °C	20±3 °C	20±3 °C	20±3 °C	20±3 °C	20±3 °C	20±3 °C	20±3 °C	20±3 °C	20±3 °C	20±3 °C	20±3 °C	20±3 °C
H34	EGSE Unit #5 (SAIU)	70,71	20±3 °C	20±3 °C	20±3 °C	20±3 °C	20±3 °C	20±3 °C	20±3 °C	20±3 °C	20±3 °C	20±3 °C	20±3 °C	20±3 °C	20±3 °C	20±3 °C	20±3 °C
H35	EGSE Unit #6 (DDL5)	72,73	20±3 °C	20±3 °C	20±3 °C	20±3 °C	20±3 °C	20±3 °C	20±3 °C	20±3 °C	20±3 °C	20±3 °C	20±3 °C	20±3 °C	20±3 °C	20±3 °C	20±3 °C
H36	EGSE Unit #7 (S/C IBU)	74,75	20±3 °C	20±3 °C	20±3 °C	20±3 °C	20±3 °C	20±3 °C	20±3 °C	20±3 °C	20±3 °C	20±3 °C	20±3 °C	20±3 °C	20±3 °C	20±3 °C	20±3 °C
H37	S/C Alt-Adapter, Top	(76,77) 78,79	DelT=0	DelT=0	DelT=0	DelT=0	DelT=0	DelT=0	DelT=0	DelT=0	DelT=0	DelT=0	DelT=0	DelT=0	DelT=0	DelT=0	DelT=0
H38	S/C Alt-Adapter, Bottom	(78,79) 80,81	DelT=0	DelT=0	DelT=0	DelT=0	DelT=0	DelT=0	DelT=0	DelT=0	DelT=0	DelT=0	DelT=0	DelT=0	DelT=0	DelT=0	DelT=0
H39	S/C Mounting System, Ring	82,83	20±3 °C	20±3 °C	20±3 °C	20±3 °C	20±3 °C	20±3 °C	20±3 °C	20±3 °C	20±3 °C	20±3 °C	20±3 °C	20±3 °C	20±3 °C	20±3 °C	20±3 °C
H40	S/C Mounting System, Clm.	85,86	20±3 °C	20±3 °C	20±3 °C	20±3 °C	20±3 °C	20±3 °C	20±3 °C	20±3 °C	20±3 °C	20±3 °C	20±3 °C	20±3 °C	20±3 °C	20±3 °C	20±3 °C
H41	S/C Mounting System, 4 Bits	99,100	20±3 °C	20±3 °C	20±3 °C	20±3 °C	20±3 °C	20±3 °C	20±3 °C	20±3 °C	20±3 °C	20±3 °C	20±3 °C	20±3 °C	20±3 °C	20±3 °C	20±3 °C

In order to observe the overall thermal balance of spacecraft, all the electronic boxes which will be normally powered-on in orbit should be powered on during the test, also. However, the total amount of power dissipation expected in orbit can not be always produced due to such constraints as related to the box's operational time limit and/or to the difficulty of realistic operation on the ground test. In this case the dissipation power shall be externally provided to those boxes. Transponder for telecommunication and equipment relevant with solar power are typical of those components, to which the predicted or measured orbit-average power (H21 to H25 at the phases of J and M in Table 1) have to be added.

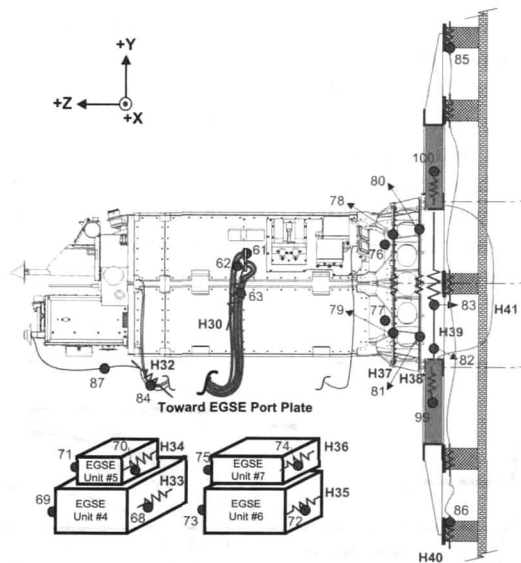


Fig. 3. Instrumentation on Ground Support Equipments (GSE)

The simulation powers to be assigned to radiators are obtained from thermal analysis of spacecraft in its operational orbit. The orbit-averaged heating values are real outcome of TRASYS(1988) run. In practicing thermal balance, these values (H1 to H20, H26, and H27, at the phases of J and M) are to be kept strictly. On the other hand, those of thermal vacuum phases are not so stringent. As mentioned before, the spacecraft should be exposed to temperature extremes during thermal vacuum cycling. The heating values can be manipulated to accelerate the spacecraft to reach at hot or cold extremes during the thermal cycling. From the phase B to phase I, and phase K to phase L, the control values for heater circuits of H1 to H27 have been generated many times to achieve the cold and hot extreme condition of spacecraft. Those data are comprehensively filed in the KOMPSAT thermal test report.

Hence the total number of heater circuits accommodated to KOMPSAT FM thermal test amounted to 66 with 25 redundant circuits included for emergency backup; 184 thermocouples of the type, 'T' were instrumented on electronic equipments as well as thermally critical locations for monitoring and control.

3. Verification of Absorbed-Flux Control Equipment

Environmental heat loads are generated by absorbed-heat flux control system. Its main functions are the real-time supplying of regulated DC electrical power to the heaters and the real-time acquisition of the thermocouple-recorded temperatures used to PID-control and to watch over if the heater is being operated within the temperature limits specified. The system is comprised of 50 linear programmable DC power supplies, fuse rack, switching unit to select remote or manual control of power supply, shunt box to exactly measure the current being impressed, and data acquisition/control units.

During the test, overheating or over-cooling the satellite may damage its electronic components which are located near the region heat-controlled. Therefore, design and operation of the control system shall be based on maintaining, first of all, the safety of the spacecraft under test and then on realizing the thermal environment as closely as possible. Delicately predicted limited powers and various software protection functions, whose consideration is imperative for the safety of spacecraft

under test, were implemented on the control system design and in setting up the spacecraft test configuration. Fuses were introduced as additional safety hardware module.

Functional demonstration of the flux control system can be found in Fig. 4. Under the vacuum less than 10^{-5} Torr and -170 °C cryogenic environment, the test was performed similarly to the spacecraft thermal cycling and balancing test. Test mockup, which was of stainless steel structure with the configuration of various mass and surface area distribution, was initially maintained at 20 °C and then lowered to -10 °C for all heat-control zones. It was lifted up 43 °C again and the similar cycling repeated. The control system was fully verified through the functional demonstration repetition and thus proven as a proper generator for the spacecraft environmental heat-loads. Its design schematic and functional verification can be thoroughly found in Kim & Cho (1999), respectively.

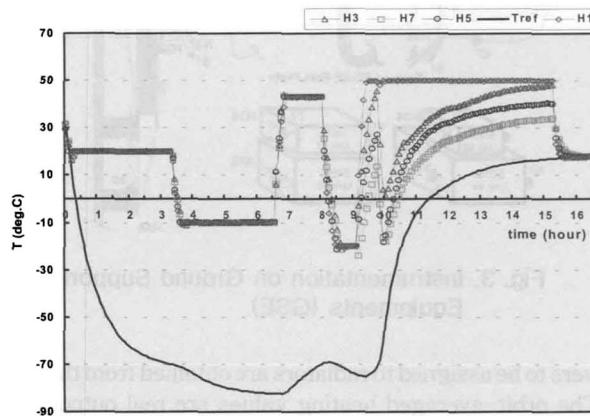


Fig. 4. Control-Function Demonstration of Flux Control Equipment.

Results Analysis and Data Reduction

1. Heat Loads Simulated through Thermal Test

The test heaters and instruments worked satisfactorily through the entire KOMPSAT thermal test. The heat loads could be controlled, just as wanted, by the absorbed-heat flux control system. The test has been performed from April 9 to April 20, 1999.

It should be noted that for all the payload radiator panels (H1, H3, H6, H9, H12, and H15), FMU (H18), and GPS receivers (H26 and H27), the original heat loads having come directly from TRASYS output were, in fact, changed to the values which Table 1 currently shows up, specifically at the cold balance phase, J. At the starting phase of cold balance the original values were put to simulate the orbit-averaged thermal environment. As time went by, however, many electronic boxes positioned on payload -Z platform approached the cold limit. To escape from such risky environmental situation, 2.6 Watts at first was added to all payload panel heaters and 2.0 Watts was added again because the prior addition was not enough to have the relevant electronics fell within acceptance limits. The similar situation has occurred to FMU and GPS receivers, and additional power was put like as the table says. Those occurrences have been caused from that the radiator area of payload panels, FMU, and GPS receivers were so large that the associated boxes lost their heat too much.

Figure 5 plots the heating power imposed through payload panel radiators from the beginning to the end of thermal test. The exhaustive control activity through all the vacuum, CPT, and balance test period is found there. Also with the concentration on the cold balance phase, the adjusting action of environmental power from the original values to the values raised by 4.6 Watts can be observed.

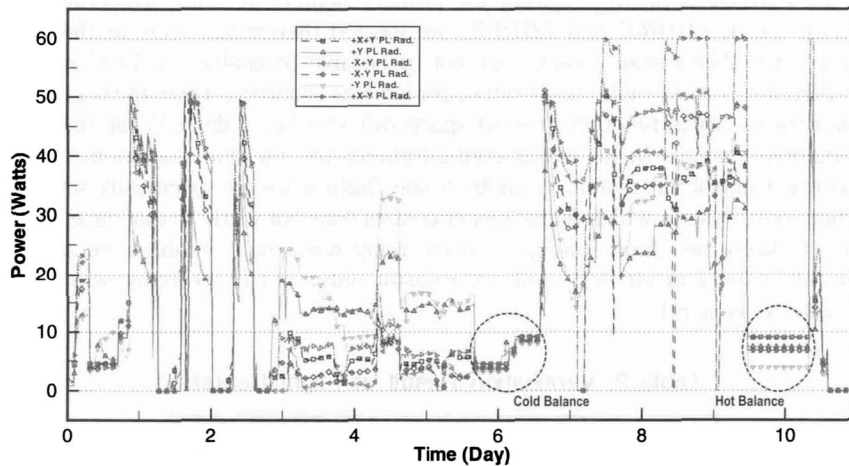


Fig. 5. Simulated Heat Loads Imposed on Payload Panel Radiators

With the consideration of corrective action taken during the cold balance, it was suggested to thermal analysis engineering that the radiator area of payload panels, FMU, and GPS receivers had to be properly reduced through aft-test model correlation. The corresponding correction to the spacecraft thermal configuration has ever been finally taken through additional MLI coverage at the spacecraft launch site.

2. Flight Heater Verification

Functioning of in-flight thermal control heaters could be verified under the vacuum/cold environment. Their checkout was performed mainly during cold transition phases and at the phases soaked by cold extreme condition. Primary heaters were almost able to be checked only at the first cold transition, and thus the second cold transition was left for redundant circuit checkout.

Table 2 is the check list of flight heater functioning. Almost all the heaters were observed to be turned on/off properly except for one set of primary/redundant heater (701HR01) located around X-band transmitter on payload -Z platform, one set of primary/redundant heater (731HR01) positioned on Zenith platform, and two redundant heaters (721HR01 and 721HR02) on Central -Z platform. They could not come on because the set points of thermostats which switch on the associated heater circuit were relatively low but the thermostats could not reach at those temperatures.

During checking out the primary heaters two primary circuits (721HR01 and 721HR02) could be observed to come on at the temperatures higher than their set points. They should not have turned on taking the temperature monitored into account if spacecraft was being operated normally. The unexpected functioning of those heaters was caused by the thermally-unfavorable spacecraft operation as explained below:

Seven (7) primary circuits out of the 26 primary and redundant flight heaters dedicated to the spacecraft bus are relay-controlled by ECU (EPS Control Unit) software. The software control refers to the temperatures sensed by flight temperature transducers. Turning-on and turning-off of those 7 heaters are ground-commandable and their set points are stored as spacecraft KPD (Key Parameter Database) values. Meanwhile single thermostat is also associated and connected to each of the ECU-controlled heater circuits (see the column of thermostat identification in Table 2). Set points of those seven thermostats are relatively higher than the points set by KPD (note: the set points listed in Table 2 come from KPD pretty much lower than the set points of single thermostat that are 10 °C to 16 °C for 701HR02 and 701HR03; 15 °C to 21 °C for 711HR01; 10 °C to 21 °C for 711HR03; 5 °C to 10 °C for 721HR01, 721HR02, and 751HR01). Purpose of those thermostats is to

protect from the burnout of heaters. During the primary heater checkout, temperatures around the SADE and SAR, which 721HR01 and 721HR02 are located thereabout, were at the level to render the singly-associated thermostats closed, but not to be able to enable the ECU relays closed. At this time, the thermally-unfavorable spacecraft operation was occurring. From the beginning of thermal vacuum cycling the electrical functional test of spacecraft was being done. While the test, spacecraft experiences multiple changes in its power configurations and mission-operation modes. In AOCS (Attitude and Orbit Control Subsystem) Standby Mode, flight software specifically sets the spacecraft to data collection-only state in which flight-heater control does not work. In that case, ECU-controlled relays continue to keep their final status, i.e., if the relay was finally enabled the associated heater would be controlled (on and off) by single thermostat only, and if the relay was finally disabled the heater would be kept off.

Table 2. Verification Result of Flight Heaters

Platform	Heater Desig.	Pri/Red	T/S Id.	Unit/Area	Turn ON Temp.(C) Required	Turn OFF Temp.(C) Required	Verification of Heater On/Off
Payload +Z	701HR04	Pri.	701TS11/12	CES, +Y	-2	6	O
		Red.	701TS13/14		-5	2	O
	701HR05	Pri.	701TS15/16	CES, -X	-2	6	O
		Red.	701TS17/18		-5	2	O
Payload -Z	701HR02	Pri.	701TS05	LRCE Base +X	0	5	O
		Red.	701TS06/07		0	8	O
	701HR03	Pri.	701TS08	EOCE Base Inbd	0	5	O
		Red.	701TS09/10		0	8	O
	701HR01	Pri.	701TS01/02	POTS Xmir, +X	-6	1	X
		Red.	701TS03/04		-10	-5	X
Nadir	711HR01	Pri.	711TS01	GRA #1/3	5	10	O
		Red.	711TS02/03		5	10	O
	711HR03	Pri.	711TS10	GRA #2, Outbd	5	10	O
		Red.	711TS08/09		5	10	O
	711HR02	Pri.	711TS04/05	RWA #4	5	10	O
		Red.	711TS06/07		-5	2	O*
Central -Z	721HR01	Pri.	721TS01	SADE Base	-10	-5	O*
		Red.	721TS02/03		-15	-10	X
	721HR02	Pri.	721TS04	SAR, +X,-Y	-10	-5	O*
		Red.	721TS05/06		-15	-10	X
RF Mod.	721HR03	Pri.	721TS07/08	GPS	5	10	O
		Red.	721TS09/10		0	8	O
Battery Mod.	751HR01	Pri.	751TS01	Battery, +Z	0	5	O
		Red.	751TS02/03		-5	2	O
MTA on Prop.	731HR01	Pri.	731TS01/02	MTA	-15	-10	X
		Red.	731TS03/04		-20	-10	X

* By an unfavorable S/C operation, the heaters could come on/off.

Proceeding with the first cold transition, during which primary heater was supposed to be checked out, the electrical power configuration of spacecraft was set to be able to check the primary heaters but its operation mode was at the AOCS standby. At earlier time of cold transition software-controlled relays had been enabled. Hence, two primary heaters (721HR01 and 721HR02) could unexpectedly come on with the associated thermostat closed, even though the flight temperature transducers were reading higher values than the turning-on KPD set-points.

This fact was noticed around the cold extreme soaking for the first cycling period and the corrective action related with the mode change has ever been taken just after the consciousness. Through the unexpected occurrence a flight-operation alert was caught out and documented for ground station usage: This was a favorable result obtained by the unfavorable spacecraft operation.

Four (4) lower (turn-on) set points out of 7 ECU-controlled heaters were coincident with the set points of their redundant heaters at the test time. This may cause simultaneous come-on of both primary and redundant heater in flight operation and thus may affect to the spacecraft power budget unfavorably. In addition to that, the simultaneous turning-on can raise very locally the temperature around the heater and can reduce the heater lifetime. In practice such simultaneous operation was witnessed during hot transitions in the test. After having scrutinized the above facts, it was strongly recommended to change the lower set points of the KPD's. Raising up the lower set points of primary heaters by 3 °C above redundant circuits was finally decided.

3. Data Reduction to the Duty Cycle and Power Consumption of Flight Heater

Duty cycle of the flight heaters could be calculated with an exhaustive analysis of the temperature

output obtained under the thermal-balanced condition. How much percentage the heater will be turning on in an operational orbit is definitively represented by the duty cycle. With the power specification of flight heaters, Table 3 lists up the data reduced to the duty cycle and converted into the orbit-averaged power. During thermal balance tests 32 Volts (31.8 Volts exactly) was streamed out to flight heaters from PCU (Power Control Unit); The bus output voltage necessarily depends upon the solar array and battery charging status in orbit and may vary from 24 to 32 Volts. It will be typically 28 Volts in the normal operation orbit. The total power calculated with 32 Volts was nearly consistent with the consumed power measured by PMTS (Power Monitoring Test Set): This means the data reduction process was very accurate.

Table 3. Flight-Heater Duty Cycles and Averaged Power Consumption Obtained from Cold/Hot Balance

Platform	HTR Desig.	Htr Spec., Watts @28V	Htr Spec., Watts @32V	Htr Duty (%) @ Balance		Average Pwr(W) w/ 28V		Average Pwr(W) w/ 32V	
				Cold	Hot	Cold	Hot	Cold	Hot
Payload +Z	701HR04	8.7	11.4	32	0	2.8	0.0	3.6	0.0
	701HR05	8.7	11.4	35	0	3.0	0.0	4.0	0.0
Payload -Z	701HR02	13.0	17.0	100	0	13.0	0.0	17.0	0.0
	701HR03	16.2	21.2	100	0	16.2	0.0	21.2	0.0
	701HR01	13.0	17.0	0	0	0.0	0.0	0.0	0.0
Nadir	711HR01	21.2	27.7	100	43	21.2	9.1	27.7	11.9
	711HR03	22.1	28.9	60	11	13.3	2.3	17.3	3.0
	711HR02	26.0	34.0	13	53	3.4	13.9	4.5	18.1
Central -Z	721HR01	13.0	17.0	0	0	0.0	0.0	0.0	0.0
	721HR02	13.0	17.0	0	0	0.0	0.0	0.0	0.0
RF Mod.	721HR03	13.0	17.0	100	100	13.0	13.0	17.0	17.0
Battery Mod	751HR01	27.0	35.3	0	0	0.0	0.0	0.0	0.0
Zenith	731HR01	13.0	17.0	0	0	0.0	0.0	0.0	0.0
Average Power of Heaters dedicated to Propulsion Subsystem						23.7	20.3	31.0	26.5
Total Power Averaged						109.6	58.6	143.2	76.5

Examining the duty cycles and averaged power in Table 3, it is indicated that the heaters located on payload -Z platform (701HR02 and 701HR03) and nadir platform (711HR01 and 711HR03) were being turned on all the time or very long time (60 to 100 % of duty cycles) under the cold balance. The nadir platform heaters, moreover, actively cycled even at the hot-balanced condition.

Returning to the Table 1 and retrieving that the simulation heat-loads under the cold balance were added by 4.6 Watts to their predetermined orbital values for payload radiators in order to boost up the relevant electronics temperature, the high duty cycles can be ascribed to the same reason as the radiator area of payload panels was so large that the enclosed have lost much of heat resulting in the cooled environment of payload module. The payload module is hexagonally enclosed by the six radiator panels with the payload platform as its top and the nadir platform as its bottom. The cold payload panels cooled down the nadir +Z platform and subsequently stole the heat out from -Z platform, by thermal conduction. That is why the heaters installed on the -Z side of nadir platform cycled that much.

It seems somewhat awkward in Table 1 that the heat loads assigned to payload radiators for cold balance are larger than those for hot balance. That is because the heat loads of hot balance were not changed from their predetermined values in order to observe again the effects of radiator size. As expected, the nadir platform heaters actively cycled at the hot balance. Whereas, the heaters positioned on -Z platform of payload module were never turned on. This is justified as follows:

As mentioned in the introduction, the hot balance is the condition at which an environmental heating and spacecraft equipment operation are maximized. The maximal usage of equipments involves a vivid payload operation. The payloads electronics are equipped on -Z payload platform. Operational powers of thermally-major electronics, which had been measured at ambient condition, were 9.6 Watts for X-band transmitter, 9.6 Watts for EEA, and 3.8 Watts for LEA, all in orbit average. During the hot balance, those powers were being generated from each boxes through the actual equipment operation and partially through the heat-loads simulation. It can be now explained that the power-off

of payload -Z platform heaters at hot balance was maintained by that the payload electronics were being powered emitting much of heat: The heat elevated the electronic box's temperature and was dissipated into the neighbor by the conduction and radiation. The flight-heater region (this term can be exactly described by the region where the thermostats and temperature transducers associated with each heater are located) was conductively heated ($\kappa \nabla T$) by the potential heat sources of electronics. Necessarily, of course, the electronics would have lost their heat via the radiative heat exchange with the cooled environment by $\sigma(T_{electronics}^4 - T_{environments}^4)$, but the amount was minor to that of the heat conducted to the heater region and thus the heaters needed not be turned on.

S-band RF assembly and GPS receivers are positioned outside of equipment closure panel. The heater, 721HR03 in Table 3 resides at between those two electronics. The panel outside is thermally costumed with MLI only except the top face of GPS receivers over which radiator of silverized mylar was applied. The cause of 100 % duty of 721HR03 can be deduced from the fact that the receivers' radiator size was so large that their temperature approached lower temperature limit; This necessitated increasing of simulated heat loads during cold balance.

Normally, spacecrafts are so thermally designed that flight heaters turn on/off with duty cycle less than 70 % in its operational orbit. Optimization of the heater duty is imperative in the light of electrical power budget, the lifetime of heaters as well as consideration of radiative property variation at EOL. Table 3 reveals the total power of spacecraft which are required for thermal control in orbit, is 109.6 Watts in the safe haven mode and 58.6 Watts in the hot science mode. This is pretty larger than the power budget allotted to spacecraft thermal subsystem. This situation was reflected on the model correlation after the test and a corrective action to the spacecraft thermal configuration has ever been taken finally.

4. Thermal-Balanced Temperatures

An equilibrium or constantly cycling temperature of the spacecraft avionics equipments could be obtained through the cold and hot balance test. Table 4 compiles those temperatures. All the components of propulsion system, though not shown in the table, could be found to cycle very frequently: The propulsion system which is attached beneath the equipment bus structure is comprised almost of mechanical components rather than electronics. This means there are rarely heat sources with it and there should be abundant flight heaters for thermal control in orbit. In case its thermal control strongly depends only on heaters the temperature cycling frequency is expected to be inevitably high.

For the other bus equipments, both of CES's thermally-cycled only under the cold balance condition; GRA's did actively cycle even under the hot balance; and LEA cycled not only under the cold but also under the hot balance.

Under the cold balance CES's could be safely kept within its operating temperature range with active cycling because it has its own heaters installed just on it. Cycling of GRA's under hot balance came directly from the large radiator size of payload panels as explained earlier. The temperature of GRA #1 (+23 °C, thermocouple #123) at cold balance was being maintained with 100 % duty cycle of the heater (711HR01) installed on it. There should be noted one fact: The heater should have been turned off if the temperature was over +10 °C (see the turning-off temperature of 711HR01 in Table 2). But the temperature reached up to +23 °C. This is because the flight temperature transducers which control the heater around GRA were positioned thermally far away from the GRA, i.e., temperature around the transducer did not reach to +10 °C even though GRA already attained the thermal equilibrium with its neighbor. It can be also imagined that this matter would be resolved by reducing the payload radiator size.

A slight deviation from the lower acceptance limit can be found with EEA. Ascribing it partially to the radiator size of payload panels, another justification can be given: The EEA was being turned off during cold balance, and its survival temperature which can be applied at the off-state of electronics spans pretty much broader (-30 to 60 °C) than the acceptance limits.

Table 4. Balanced Temperatures at Cold/Hot Thermal Equilibrium

Pltfm	Location	Temp. Limit (°C)		TC #	Balanced Temp. (°C)	
		Low. Red.	Up. Red.		At Cold Bal.	At Hot Bal.
Payload Pltfm +Z	X-Band Antenna	-100	100	176	-81	-66
	ESA, Rad. Upper	**	**	177	-24 to -15	-8 to -6
	ESA, Rad. Lower	**	**	178	-43	-29
	ESA, Foot Brkt	N/A	N/A	179	-3	+8
	LSA, Scan Assy	**	**	181	+1	+3
	LSA, Thermostat	**	**	182	+1	+3
	LSA, Foot Brkt			183	-1	+2
	FMU	-10	50	35	-7	+6
	SPS Foot Brkt	-11	51	185	-10	+5
	CES +Y	-5	40	38	+11 to +29	+38
	CES -X	-5	40	40	+10 to +28	+32
	FSS, +X	-24	61	186	-10	+1
Payload Pltfm -Z	LEA *	0	45	167	-2.5 to -2	+1.5 to +2.5
	Xmitter, +X	-10	50	42	-7	+19
	X-band Xmtr, B	-10	50	168	-5	+1
	CESE	-5	50	170	-5	+11
	EEA *	0	45	171	-3 ***	+7
	X-Band RF Assy	-10	50	172	-6	+6
Nadir Pltfm	GRA #1 Bracket	5	55	123	+23	+11 to +25
	GRA #2	5	55	124	+10 (9.9 to 10.5)	+10 (9.8 to 10.6)
	GRA #3	5	55	188	+6	+7 to +10
	RWA #1	-5	55	126	+3	+8
	RWA #2	-5	55	127	+1	+8
	RWA #3	-5	55	189	-2	+5
	CEA	-20	55	129	-2	+9
Central Pltfm +Z	ECU, A	-20	55	130	-5	+6
	ECU, B	-20	55	131	+1	+4
	RDU, A	-20	55	132	-4	+7
	RDU, B	-20	55	133	+3	+7
	PCU	-20	50	134	+4	+10
	OBC	-20	55	135	0	+9
Central Pltfm -Z	SAR #1	-20	50	46	+3	+10
	SAR #2	-20	50	48	+5	+10
	DDC	-20	50	140	-3	+6
	SADA, +Y	-15	55	141	-7	+2
	VDE	-20	55	142	-6	+2
	SADE	-20	55	143	-1	+6
	Xpndr, +X	-20	55	44	0	+15
	Xpndr, B	-20	55	144	+1	+6
Battery, etc.	TAM, A	-25	55	145	-11	-4
	Batt. Inside, Top	-5	20	146	+1	+9
	Batt. Inside, Btm.	-5	20	147	+1	+9
	RF Assy, S-Band	-20	55	156	-6	+1
	GPS Receiver A	-10	50	51	-8	-7
	GPS Receiver B	-10	50	54	-7	-5
MTA #1	-75	75	158	-15	-10	

* Lower / Upper Survival Temperatures of both EEA and LEA are -30 / 60 °C.
 ** The limits vary with zone to zone and with the operation mode.
 *** During the cold balance, EEA was OFF. This temperature deviation is acceptable considering the survival temperature range.

Summary and Conclusions

Comprehensive data analysis for the KOMPSAT thermal test results was given. Reviewed and discussed are contents as follows:

- 1) Thermal test configuration implemented on KOMPSAT spacecraft bus was explained in detail.
- 2) Absorbed-heat flux method for the simulation of orbital environment of spacecraft was demonstrated with its equipment verification results.
- 3) Functional verification of flight heater was presented with concurrent description on the spacecraft operation mode.
- 4) Reduction of temperature data to the heater duty cycle and its conversion to the electrical power were discussed.
- 5) Thermal-balanced temperatures of the spacecraft equipments were listed and commented with the inter-relation to heater duty cycle.

A guideline for the aft-test model correlation was qualitatively given as a consequence of data analysis.

References

- Gilmore, D. G., 1994, *Satellite Thermal Control Handbook*, The Aerospace Corporation Press, California, USA
- Kim, J. S. and Cho, J. H., 1998, "Satellite Test Design for the Simulation of Orbital Thermal Environment," *Proceedings of the KSAS Fall Annual Meeting*, pp. 498-501
- Kim, J. S. and Cho, J. H., 1999, "Employment of Absorbed-Heat Flux Method for the Simulation Test of KOMPSAT Orbital Thermal Environment," *Proceedings of the KSAS Spring Annual Meeting*, pp. 620-623
- Kim, J. S., Cho, J. H., and Choi, J. M., 1996, "A Study on the Simulation Test of Satellite-Orbit Environment (I): T/V Chamber for Space Simulation," *Proceedings of KSAS Spring Annual Meeting*, pp. 419-422
- MIL-STD-1540B, 1982, "Test Requirements for Space Vehicles," *US Air Force Military Standard*
- TRASYS, 1988, "Thermal Radiation Analyzer System," Johnson Space Center, NASA, USA

Acronyms

AOCS	Attitude & Orbit Control Subsystem	LEA	LRC Electronics Assembly
BOL	Beginning-of-Life	LEO	Low Earth Orbit
CEA	Control Electronics Assembly	LRC	Low Resolution Camera
CES	Conical Earth Sensor	LSA	LRC Sensor Assembly
CESE	CES Control Electronics	MGSE	Mechanical Ground Support Equip.
CPT	Comprehensive Performance Test	MLI	Multi Layer Insulation
DDC	Deployment Device Controller	OBC	On-board Computer
ECU	EPS Control Unit	OSC	Orbital Science Corp. (USA)
EEA	EOC Electronics Assembly	PCU	Power Control Unit
EGSE	Electrical Ground Support Equipment	PFM	Proto-Flight Model
EOC	Electro-Optical Camera	PMTS	Power Monitoring Test Set (an EGSE)
EOL	End-of-Life	RDE	Responsible Design Engineer
EPS	Electrical Power Subsystem	RDU	Remote Drive Unit
ESA	EOC Sensor Assembly	RWA	Reaction Wheel Assembly
FM	Flight Model	SADA	Solar Array Drive Assembly
FMU	Flux Modulation Unit	SADE	Solar Array Drive Electronics
FSS	Fine Sun Sensor	SAR	Solar Array Regulator
GPS	Global Positioning System	SPS	Science Physics Sensor
GRA	Gyro Reference Assembly	SSM	Second Surface Mirror
KPD	Key Parameter Database	VDE	Valve Drive Electronics